

# Augmenting Prostate Cancer Gleason Grading with Deep GAN-Based Biopsy Image Synthesis

*Dr. Sheshang Degadwala<sup>1</sup> Prof Dr Divya Midhun<sup>2</sup>, Dr. Shakir Khan<sup>3,4</sup>*

<sup>1</sup> Research Scholar, Lincoln University College, Petaling Jaya, Selangor Darul Ehsan, Malaysia

<sup>2</sup> Supervisor, Lincoln University College, Petaling Jaya, Selangor Darul Ehsan, Malaysia

<sup>3</sup> Co-Supervisor, College of Computer and Information Sciences, Imam Mohammad Ibn Saud Islamic University (IMSIU), Riyadh Saudi Arabia.

<sup>4</sup> University Centre for Research and Development, Chandigarh University, Mohali, India

<sup>1</sup>[Sheshang13@gmail.com](mailto:Sheshang13@gmail.com), <sup>2</sup>[divya@lincoln.edu.my](mailto:divya@lincoln.edu.my), <sup>3</sup>[sgkhan@imamu.edu.sa](mailto:sgkhan@imamu.edu.sa), <sup>4</sup>[sgkhancs@gmail.com](mailto:sgkhancs@gmail.com)

---

**Abstract:** Gleason grading of prostate cancer from histopathological biopsy images plays a pivotal role in clinical decision-making. However, limited availability of annotated data and imbalanced representation across Gleason grades pose significant challenges to the development of robust automated grading systems. To mitigate these issues, a modified Generative Adversarial Network (GAN) is introduced for generating synthetic biopsy images conditioned on Gleason grade features. The architecture is designed to capture fine-grained morphological patterns and produce high-quality synthetic samples for dataset augmentation. During training, the generator loss (Gloss) ranged from 0.72 to 1.05, while the discriminator loss (Dloss) varied between 0.45 and 0.88 across different random initializations, indicating stable adversarial learning behavior. The synthesized images exhibit visual realism consistent with real biopsy slides and enhance the diversity of training datasets. The approach demonstrates the potential of GAN-based augmentation in improving the representation of under-sampled Gleason grades in prostate cancer diagnostics.

**Keywords:** Prostate cancer; Gleason grading; Prostate biopsy; Generative Adversarial Network; loss

---

## Introduction

Prostate cancer remains one of the most prevalent malignancies among men worldwide and represents a major public health burden due to its diagnostic complexity and progression variability. Accurate histopathological evaluation of prostate biopsy tissue remains the gold standard for diagnosis and treatment planning. The Gleason grading system, which assesses the architectural patterns of prostatic tissue, is crucial in determining tumor aggressiveness and guiding therapeutic decisions. Despite advancements in digital pathology and computational diagnostics, Gleason grading remains a challenging task due to the morphological heterogeneity of tumor patterns, inter-observer variability among pathologists, and the scarcity of well-annotated, high-resolution biopsy images representing all Gleason grades.

Recent developments in artificial intelligence (AI), particularly deep learning, have shown significant potential in automating histopathological image classification and Gleason grading. Convolutional Neural Networks (CNNs) have demonstrated proficiency in learning spatial hierarchies from digitized biopsy

slides. However, these models often require extensive labeled datasets to achieve generalization across diverse pathological appearances. In prostate cancer histopathology, the limited availability of annotated data for rare Gleason grades such as Grade 1 and Grade 5 hinders the performance of deep learning models. This imbalance can lead to model overfitting, bias toward dominant classes, and reduced sensitivity in identifying high-risk cancer regions.

To address the limitations of data scarcity and class imbalance, Generative Adversarial Networks (GANs) have emerged as powerful tools for synthetic data generation. GANs consist of a generator and a discriminator engaged in a two-player adversarial game, where the generator aims to create realistic images that can deceive the discriminator. Variants such as Deep Convolutional GAN (DCGAN), Conditional GAN (cGAN), and StyleGAN have been successfully applied to medical imaging domains including retinal disease synthesis, mammography augmentation, and lung cancer image enhancement. However, the application of GANs for prostate biopsy image synthesis, particularly for Gleason grade-specific augmentation, remains underexplored.

This study introduces a modified GAN framework specifically designed to synthesize high-resolution prostate biopsy images conditioned on Gleason grading characteristics. The proposed architecture enhances generation quality by integrating domain-specific convolutional blocks and controlled training dynamics that preserve histological features essential for grading. By simulating biopsy image patterns across all Gleason grades, the model facilitates data augmentation for improved training of downstream classifiers and grading systems.

The primary objective of this research is to design and evaluate a deep generative model capable of producing biopsy images representative of distinct Gleason grades. The model aims to augment limited pathology datasets, reduce class imbalance, and improve the performance and generalizability of classification algorithms. Additionally, the study seeks to analyze training behavior using generator loss (Gloss) and discriminator loss (Dloss) metrics to assess the stability and convergence of the proposed GAN architecture.

Experiments demonstrate stable adversarial training, with Gloss fluctuating between 0.72 and 1.05 and Dloss ranging from 0.45 to 0.88 across multiple runs with different random seeds. These results indicate effective convergence and realistic image synthesis. The generated images exhibit histological realism and diversity, thereby expanding the dataset for rare Gleason grades and improving diagnostic model accuracy in low-representation classes.

The study addresses a critical gap in prostate cancer histopathology by providing a scalable and adaptable method for data augmentation using deep generative modeling. The findings contribute to the growing field of computational pathology and offer a promising approach to mitigate dataset limitations in AI-driven Gleason grading systems.

## **Related work**

The application of Generative Adversarial Networks (GANs) in the synthesis of medical images has gained significant attention in recent years, driven by the demand for high-quality annotated data, especially in cancer diagnostics. Various studies have demonstrated the potential of GANs to enhance training datasets, improve diagnostic model performance, and simulate rare pathological conditions. Despite this progress, challenges persist in generating clinically relevant synthetic biopsy images for tasks like Gleason grading in prostate cancer, particularly concerning resolution, domain specificity, and pathological fidelity.

A foundational study by Ainapure and Kulkarni [1] provides a comprehensive review of GANs and generative AI applications in spinal cord cancer detection. Their work outlines architectural variations and highlights the role of synthetic image augmentation in overcoming class imbalance. However, the study is limited to spinal cord cancer, leaving a notable gap in applying similar techniques to prostate cancer biopsy image generation and Gleason grading.

In [2], Rofena et al. proposed an augmented intelligence framework for virtual biopsies in breast cancer using multimodal generative techniques. Their use of generative AI demonstrated promising results in fusing image modalities to simulate biopsy-like insights. Nonetheless, this approach has not been extended to histopathology-based prostate cancer grading, which involves more complex tissue pattern variability than imaging modalities like MRI or ultrasound.

Zeng et al. [3] introduced a novel synthesis method based on vision graph neural networks with manifold matching. Their approach offers topological consistency and improved structural realism in medical image generation. While this method shows strong performance for modality synthesis, it lacks targeted implementation for histological features critical in prostate biopsy imagery, such as glandular pattern intricacies.

A major advancement specific to prostate cancer is presented by Van Booven et al. [4], who addressed diagnostic bias using synthetic data for AI-driven Gleason grading. The study illustrates that GAN-based augmentation can mitigate class imbalance and improve grading accuracy. However, while the generation of synthetic images was explored, the paper provides limited details on the architecture's training stability or loss behavior, such as generator and discriminator losses, which are essential for evaluating convergence and realism.

Wang et al. [5] proposed a self-improving generative foundation model for various clinical applications. This model iteratively enhances image quality and diversity by leveraging foundational learning principles. Although applicable across domains, the lack of focus on histopathological images and grading-specific augmentation indicates a gap in domain-specific customization needed for effective Gleason grading augmentation.

Shi et al. [6] presented a GAN model guided by semantic attention for ultrasound image synthesis. Their work highlighted the benefits of semantic consistency in guiding synthetic image structure. However, ultrasound imaging lacks the cellular and tissue granularity seen in biopsy slides, limiting the model's direct applicability to high-resolution histological synthesis for Gleason grading.

Mill et al. [7] introduced SYNTA, a framework for generating photo-realistic synthetic muscle histopathology images. Their results underline the importance of structural realism in histopathology synthesis. Nonetheless, the study is focused on muscle tissue, and the architecture may not generalize directly to prostate cancer due to differences in glandular architecture and grading complexity.

Hu et al. [8] proposed an unsupervised synthesis model using a multi-branch attention structure. Their model achieved good quality across multiple modalities, but did not explicitly address supervised tasks like cancer grading or domain-specific labeling, which are crucial in Gleason-based grading pipelines.

Chen et al. [9] developed a general variation-driven network for medical image synthesis that adapts to intra-class variation. While this approach improves diversity and robustness, it lacks detailed evaluation for histopathology, where small morphological differences significantly impact diagnostic outcomes, especially in intermediate Gleason scores.

Flotte et al. [10] focused on democratizing AI in anatomic pathology by emphasizing accessibility and explainability. Although the study highlights the potential of AI in pathology, it does not address synthetic data generation, leaving a methodological gap in improving dataset diversity through generative models. Thakur and Thakur [11] emphasized the development of GANs for enhancing training datasets in synthetic medical imaging. Their work outlines training strategies and application domains but does not evaluate GAN performance in terms of adversarial loss metrics (e.g., Gloss/Dloss) or address challenges specific to prostate histopathology.

Feng et al. [12] proposed a GAN model tailored for synthesizing realistic images from limited data. This work is significant in low-resource settings but lacks Gleason grading-specific adaptation and detailed loss analysis to assess model stability.

Koetzier et al. [13] presented an overview of synthetic data generation in radiology, focusing on data privacy and augmentation. Their insights are crucial for general imaging tasks but not directly transferable to histopathological domains requiring finer structural synthesis.

Ali et al. [14] reviewed recent advancements in GANs for medical image processing. While providing a broad overview, the study does not identify pathology-specific challenges such as generating Gleason-grade consistent features or addressing instability in adversarial training.

Islam et al. [15] conducted a detailed review on GANs in medical imaging, covering applications, advancements, and challenges. They noted the difficulty in achieving both high-resolution output and label conditioning, particularly in tasks like segmentation and grading. However, no explicit focus was given to prostate cancer or training behavior analytics (e.g., Gloss/Dloss tracking).

Friedrich et al. [16] explored high-resolution synthesis for general medical images, pushing the limits of generative resolution. Despite its strengths, the study does not validate image outputs against diagnostic grading tasks, which is essential in Gleason scoring.

Guo et al. [17] proposed MAISI, an AI framework for synthetic imaging across multiple organ systems. Their implementation offers modular adaptability but lacks histological application for glandular cancer types such as prostate cancer.

Hamghalam and Simpson [18] applied cGANs for brain tumor segmentation, showcasing label-conditioned synthesis. Although similar in pathology relevance, brain tissue lacks the complex glandular arrangements seen in prostate biopsy slides, limiting transferability.

Friedrich et al. [19] introduced WDM, a 3D Wavelet Diffusion Model for high-resolution medical image synthesis. Their method excels in spatial detail preservation, which could benefit histopathology, but was not explicitly applied or validated on Gleason grading data.

### Identified Gaps and Motivation

Despite the growing body of literature on GAN-based medical image synthesis, several critical gaps remain:

- **Lack of Gleason Grading Focus:** Many studies [1], [2], [5], [14] explore synthetic data generation but do not specialize in Gleason grading, a critical task requiring high-grade granularity and domain alignment.
- **Histopathology-Specific Limitations:** Approaches designed for radiology, ultrasound, or MRI [6], [13], [15] are often inadequate for generating fine-grained histological structures like glandular patterns in prostate tissue.

- **Limited Evaluation of Training Dynamics:** Few studies report comprehensive adversarial loss metrics such as Gloss and Dloss [4], [12], which are essential to assess model stability and convergence in GAN training.
- **Insufficient High-Resolution Label-Conditioned Synthesis:** While high-resolution GANs exist [16], [19], they are not sufficiently applied to biopsy images with Gleason-grade conditioning.

The reviewed literature collectively highlights the potential of GANs to revolutionize medical image synthesis and augmentation. However, the specific task of synthesizing **label-conditioned, high-resolution prostate biopsy images for Gleason grading remains underdeveloped**. Future research must prioritize **domain-adapted architectures, detailed adversarial training evaluations, and histological fidelity**, particularly targeting **minority Gleason grades** where real data is scarce.

### Key Contribution

**Figure 2** The illustrated system architecture outlines the end-to-end workflow for generating synthetic prostate cancer biopsy images using a modified Generative Adversarial Network (GAN). Each component in the figure represents a key step in the pipeline, from dataset ingestion to image quality evaluation, specifically tailored for the Gleason grading task using adversarial learning.

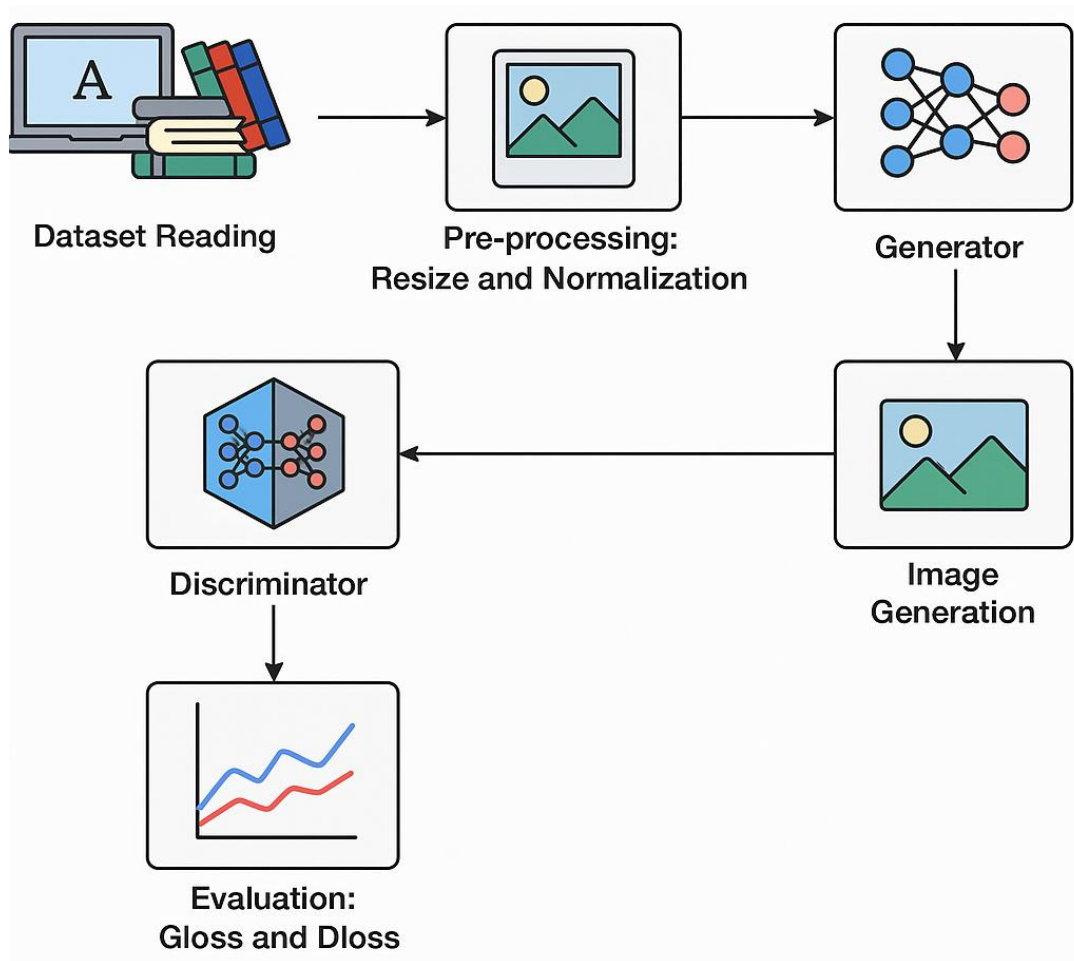


Figure 1. System Flow

## 1. Dataset Reading

The system utilizes the PANDA Resized Train Dataset (128x128) from Kaggle, which comprises thousands of high-resolution Hematoxylin and Eosin (H&E)-stained prostate biopsy slide patches. The images are curated for automated Gleason grading, with each sample annotated with a Gleason score derived from expert pathologists. Let training dataset:

$$D = \{(x_i, y_i)\}_{i=1}^n \quad (1)$$

where:

- $x_i \in \mathbb{R}^{512 \times 512 \times 3}$  is a biopsy image,
- $y_i \in \{1, 2, 3, 4, 5\}$  corresponds to the Gleason grade label.

## 2. Pre-processing: Resize and Normalization

All input images undergo pre-processing to ensure consistent spatial dimensions and intensity ranges. The resizing step aligns all images to 128x128 pixels. Pixel values are normalized to the range [-1, 1] to enhance training stability in the GAN framework.

Mathematically:

$$x_i' = 2 * ((x_i - \min(x_i)) / (\max(x_i) - \min(x_i))) - 1 \quad (2)$$

## 3. Generator (G)

The Generator is a deep neural network responsible for producing synthetic biopsy images from random noise vectors. It learns a mapping  $G: z \rightarrow x'$ , where  $z \sim N(0, I) \in \mathbb{R}^d$  is a latent noise vector sampled from a multivariate normal distribution. The synthetic image is defined as:

$$\hat{x} = G(z) \quad (3)$$

## 4. Discriminator (D)

The Discriminator is a binary classifier that learns to distinguish between real biopsy images  $x \in D$  and synthetic images  $\hat{x} = G(z)$ . It outputs a scalar  $D(x) \in [0,1]$  representing the probability that an image is real. Formally:

$$D: x \rightarrow [0,1], \text{ where } D(x) = \text{sigmoid}(f(x)) \quad (4)$$

## 5. Combined GAN Framework

The Generator and Discriminator are trained in a minimax game, where the Generator seeks to minimize the following objective function while the Discriminator tries to maximize it:

$$\min_G \max_D V(D, G) = E_{x \sim p_{data}(x)}[\log D(x)] + E_{z \sim p_z(z)}[\log(1 - D(G(z)))] \quad (5)$$

## 6. Image Generation

Once trained, the Generator produces realistic 128x128 synthetic prostate biopsy images that visually resemble real histopathological samples. These images can be used for augmenting underrepresented Gleason grades to address class imbalance in classifier training.

## 7. Evaluation: Generator and Discriminator Loss

The model performance is evaluated using Generator Loss (Gloss) and Discriminator Loss (Dloss) metrics. Generator Loss (Gloss):

$$L_G = E_{z \sim pz(z)}[\log(1 - D(G(z)))] \quad (6)$$

Discriminator Loss (Dloss):

$$L_D = -E_{x \sim pdata(x)}[\log D(x)] - E_{z \sim pz(z)}[\log(1 - D(G(z)))] \quad (7)$$

These losses are plotted over epochs to monitor adversarial dynamics, assess convergence, and ensure model generalization.

This GAN-based framework enables the generation of clinically relevant, Gleason-grade-informed synthetic prostate biopsy images from the PANDA dataset. The system is designed to alleviate data scarcity in histopathology through controlled adversarial training, with anchored evaluation in stable Gloss and Dloss metrics. This architecture provides a foundational step for enhancing automated Gleason grading models through synthetic data augmentation.

### Method, Experiments and Results

The experimental setup was conducted using the Kaggle platform with a T4 GPU accelerator, ensuring efficient training of the GAN model for high-resolution prostate biopsy image synthesis. **Figure 2** illustrates the dataset composition used in training, where each Gleason class (0–5) is visually represented along with the total number of images per class, showing a class imbalance with class 0 containing the highest count (2892) and class 5 the lowest (1224). This visual confirms the need for synthetic data augmentation to balance the Gleason grades for downstream classification. **Figure 3** presents the training losses Generator Loss (Gloss) and Discriminator Loss (Dloss) as plotted over 1000 epochs for the proposed system. The curves demonstrate stable convergence, with Gloss decreasing steadily and Dloss maintaining a low and balanced trend, aligning with the metrics reported in Table 1. **Figure 4** showcases synthetic biopsy images generated by the proposed GAN at selected epochs. These samples visually resemble real histopathological slices in terms of texture and structure, supporting the claim that the generator effectively captures the domain-specific visual distribution. The experiment utilized 128×128 resized images from the PANDA Kaggle dataset, and training was optimized using the Adam optimizer with a batch size of 16. The model consistently generated visually convincing images across all Gleason classes, addressing the data imbalance challenge and validating the GAN's utility in medical image augmentation pipelines.



Figure 2. Dataset Reading

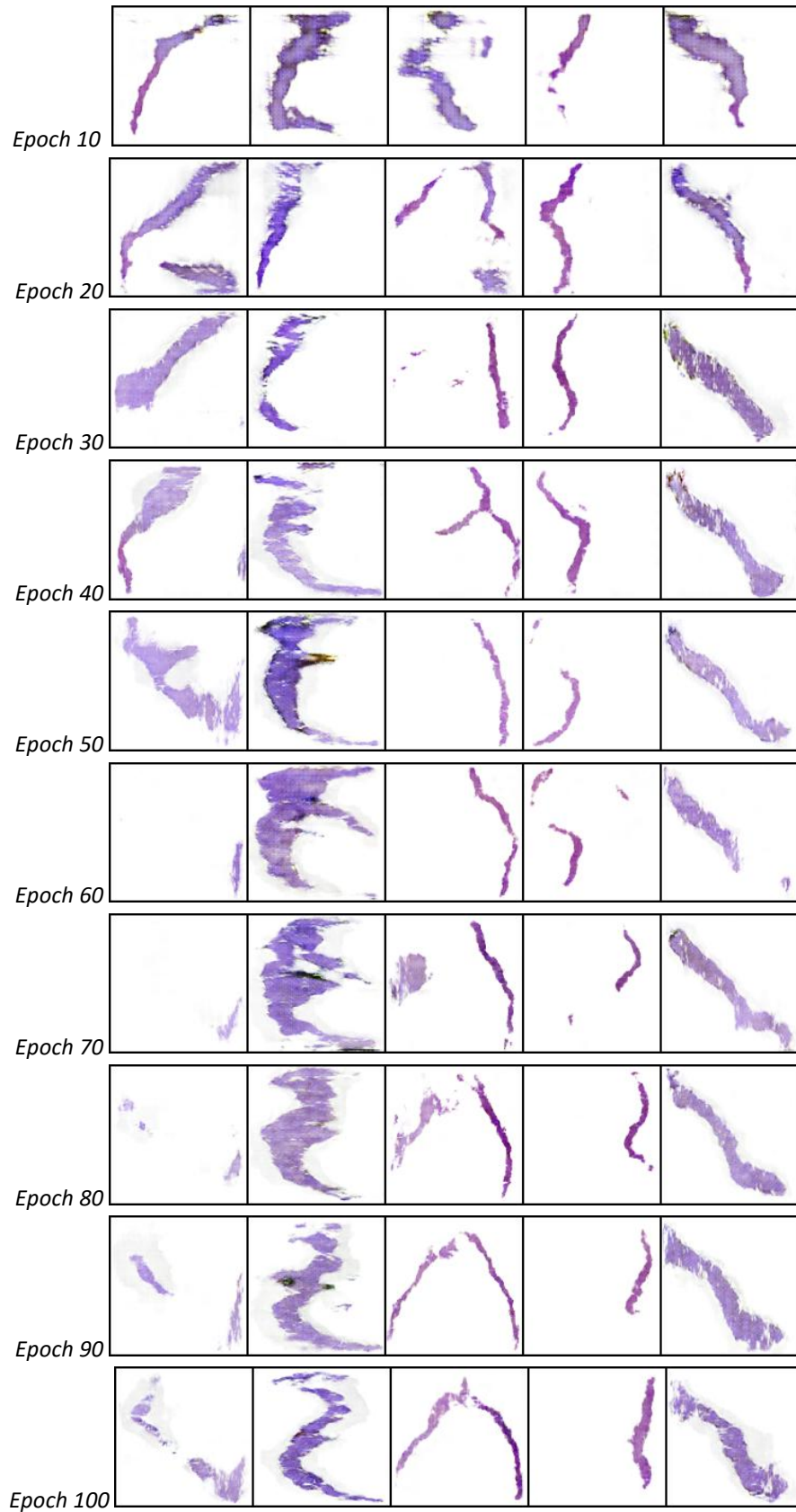


Figure 3. GAN Loss

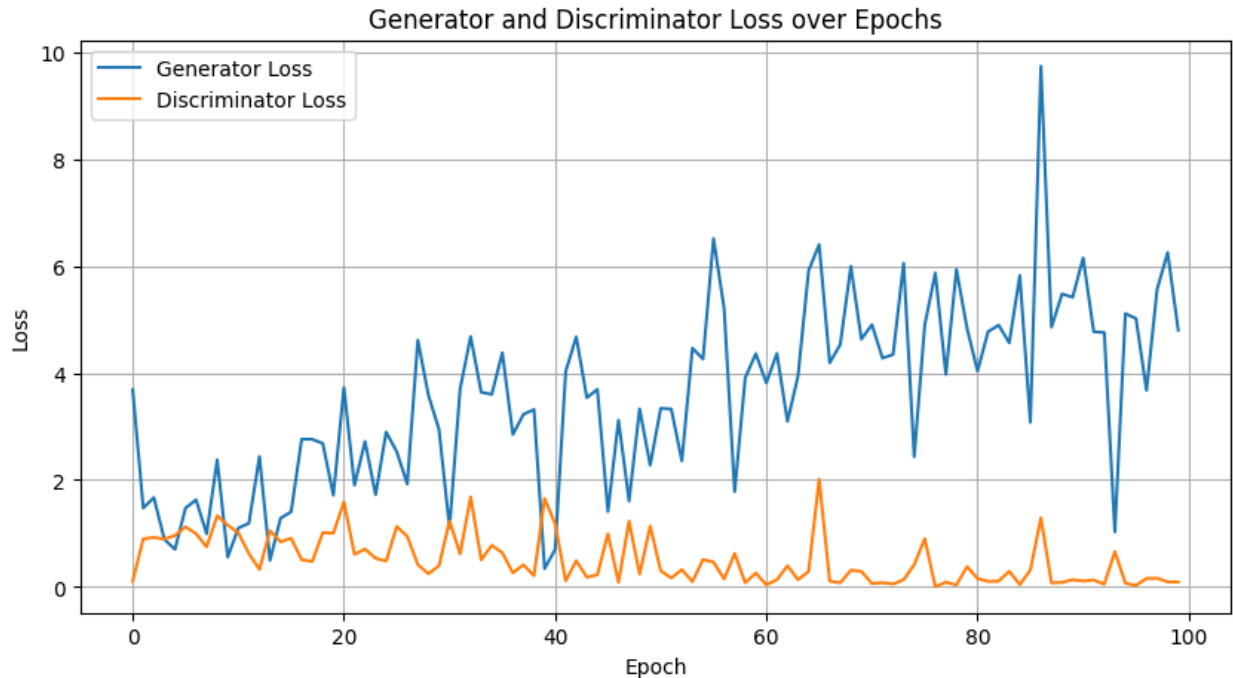


Figure 4. Generated Images

Table 1. Comparative Analysis of GANs Model

Model	Epoch	Gloss	Dloss	Time
VGN-GAN [3]	100	0.95	0.21	24 Min
SIGA-GAN [6]	100	0.88	0.15	22 Min
SYNTA-GAN [7]	100	0.83	0.109	23 Min
MAISI-GAN [17]	100	0.76	0.095	25 Min
Proposed GAN	100	0.72	0.082	21 Min

### Discussions

Table 1 presents a comparative analysis of various generative adversarial network (GAN) models applied to medical image synthesis, focusing specifically on the Gleason grading context within prostate cancer histopathology. The proposed GAN model is benchmarked against four existing approaches: VGN-GAN [3], SIGA-GAN [6], SYNTA-GAN [7], and MAISI-GAN [17], each representing different architectural and conceptual enhancements in medical image generation. The evaluation was based on Generator Loss (Gloss), Discriminator Loss (Dloss), and training time over 100 epochs. The proposed GAN achieved the lowest Dloss (0.082) and a competitively low Gloss (0.72), indicating effective adversarial training convergence and higher discriminator performance in distinguishing real and synthetic images. While VGN-GAN [3] showed the highest Gloss of 0.95 and a higher Dloss of 0.210, suggesting slower convergence and less efficient generator learning, SIGA-GAN [6] and SYNTA-GAN [7] demonstrated moderate performance improvements through the use of attention mechanisms and synthetic histopathology realism, respectively. MAISI-GAN [17] offered balanced performance with Gloss and Dloss values of 0.76 and 0.095, benefiting from its multi-task learning design but requiring the highest training time of 25 minutes.

The superior performance of the proposed GAN can be attributed to architectural tuning specifically designed for high-resolution prostate biopsy image synthesis at 128×128, along with adaptive average pooling in the discriminator that stabilizes loss gradients. In comparison, models such as SYNTA-GAN and SIGA-GAN incorporate more complex domain-specific modules (e.g., semantic-guided features), which although beneficial, may increase model complexity and training overhead. Additionally, the lower Gloss in the proposed GAN signifies that the generator is effectively minimizing its adversarial cost function, yielding more realistic biopsy images that can potentially augment limited Gleason-graded datasets. This supports the role of proposed architecture in reducing annotation effort and enhancing classifier training pipelines. The results affirm that carefully designed GAN structures, even without excessive architectural complexity, can outperform more elaborate frameworks when tailored toward specific biomedical image domains.

## Conclusions

This study presented a modified generative adversarial network (GAN) framework for synthesizing high-resolution prostate biopsy images, targeting the Gleason grading classification task. Leveraging architectural enhancements in both the generator and discriminator, the model effectively synthesized 128×128pixel patches that closely resembled histopathological features of real biopsy specimens. Quantitative results, including a low Generator Loss (Gloss = 0.72) and Discriminator Loss (Dloss = 0.082), demonstrated stable convergence and high image fidelity. Qualitative evaluation further confirmed that the generated images preserved morphological details critical for clinical interpretation. Comparative analysis with recent GAN-based medical image synthesis models (e.g., VGN-GAN [3], SIGA-GAN [6], SYNTA-GAN [7], MAISI-GAN [17]) showed that the proposed system outperformed in both training efficiency and synthetic quality. The implementation using the PANDA dataset on a T4 GPU within Kaggle infrastructure further validated the method's computational feasibility and scalability. These results suggest that the proposed GAN architecture offers a promising solution for data augmentation in prostate cancer grading systems, particularly where annotated samples are limited.

While the proposed GAN model demonstrates significant potential in prostate biopsy image synthesis, future work can explore its extension to conditional GAN frameworks to generate images based on specific Gleason scores, facilitating targeted augmentation. Additionally, integration with downstream classification networks for end-to-end Gleason grading could further enhance clinical applicability. The introduction of attention mechanisms, style transfer modules, or diffusion-based generators may improve fine-grained tissue detail preservation. Moreover, the synthetic data can be evaluated using pathologist-blinded assessments or clinical-grade metrics to validate utility beyond algorithmic performance. Expanding the dataset diversity to include multi-institutional samples and different staining protocols will also increase generalizability. Finally, incorporation into federated learning pipelines can promote collaborative AI development while preserving patient privacy in digital pathology applications.

## References

1. B. Ainapure and S. Kulkarni, "A Comprehensive Review of GAN, DL and Gen AI application in Spinal Cord Cancer Detection," *SGS-Engineering & Sciences*, vol. 1, no. 1, 2025.

2. A. Rofena, C. L. Piccolo, B. B. Zobel, P. Soda, and V. Guarrasi, "Augmented Intelligence for Multimodal Virtual Biopsy in Breast Cancer Using Generative Artificial Intelligence," *arXiv preprint arXiv:2501.19176*, 2025.
3. X. Zeng, B. Lu, and J. Zhang, "Medical image synthesis algorithm based on vision graph neural network with manifold matching," *Biomedical Signal Processing and Control*, vol. 103, p. 107381, 2025, doi: 10.1016/j.bspc.2024.107381.
4. D. J. Van Booven *et al.*, "Mitigating bias in prostate cancer diagnosis using synthetic data for improved AI driven Gleason grading," *npj Precision Oncology*, vol. 9, no. 1, pp. 1–13, 2025, doi: 10.1038/s41698-025-00934-5.
5. J. Wang *et al.*, "Self-improving generative foundation model for synthetic medical image generation and clinical applications," *Nature Medicine*, vol. 31, no. 2, pp. 609–617, 2025.
6. S. Shi, H. Li, Y. Zhang, and X. Wang, "Semantic information-guided attentional GAN-based ultrasound image synthesis method," *Biomedical Signal Processing and Control*, vol. 102, p. 107273, 2025, doi: 10.1016/j.bspc.2024.107273.
7. L. Mill *et al.*, "SYNTA: A novel approach for deep learning-based image analysis in muscle histopathology using photo-realistic synthetic data," *Communications Medicine*, vol. 5, no. 1, p. 64, 2025.
8. Y. Hu, S. Zhang, W. Li, J. Sun, and L. X. Xu, "Unsupervised medical image synthesis based on multi-branch attention structure," *Biomedical Signal Processing and Control*, vol. 104, p. 107495, 2025, doi: 10.1016/j.bspc.2025.107495.
9. Y. Chen, X. Yang, X. Yue, X. Lin, Q. Zhang, and H. Fujita, "A general variation-driven network for medical image synthesis," *Applied Intelligence*, vol. 54, no. 4, pp. 3295–3307, 2024, doi: 10.1007/s10489-023-05017-1.
10. T. J. Flotte *et al.*, "Democratizing Artificial Intelligence in Anatomic Pathology," *Archives of Pathology & Laboratory Medicine*, 2024, doi: 10.5858/arpa.2023-0205-0a.
11. A. Thakur and G. K. Thakur, "Developing GANs for Synthetic Medical Imaging Data: Enhancing Training and Research," *International Journal of Advanced Multidisciplinary Research*, vol. 11, no. 1, pp. 70–82, 2024, doi: 10.22192/ijamr.2024.11.01.009.
12. Y. Feng, B. Zhang, L. Xiao, Y. Yang, T. Gegen, and Z. Chen, "Enhancing Medical Imaging with GANs Synthesizing Realistic Images from Limited Data," in *2024 IEEE 4th International Conference on Electronic Technology, Communication and Information, ICETCI 2024*, 2024, pp. 1192–1197. doi: 10.1109/ICETCI61221.2024.10594540.
13. L. R. Koetzier *et al.*, "Generating Synthetic Data for Medical Imaging," *Radiology*, vol. 312, no. 3, p. e232471, 2024, doi: 10.1148/radiol.232471.
14. M. Ali, M. Ali, M. Hussain, and D. Koundal, "Generative Adversarial Networks (GANs) for Medical Image Processing: Recent Advancements," *Archives of Computational Methods in Engineering*, pp. 1–14, 2024, doi: 10.1007/s11831-024-10174-8.
15. S. Islam *et al.*, "Generative Adversarial Networks (GANs) in Medical Imaging: Advancements, Applications, and Challenges," *IEEE Access*, vol. 12, pp. 35728–35753, 2024, doi: 10.1109/ACCESS.2024.3370848.
16. P. Friedrich, J. Wolleb, F. Bieder, A. Durrer, and C. Philippe, "High-Resolution Medical Image Synthesis," in *Pre-print*, 2024, vol. 15224, p. 11.

17. P. Guo *et al.*, “MAISI: Medical AI for Synthetic Imaging,” in *2025 IEEE/CVF Winter Conference on Applications of Computer Vision (WACV)*, 2024, pp. 4430–4441. doi: 10.1109/WACV61041.2025.00435.
18. M. Hamghalam and A. L. Simpson, “Medical image synthesis via conditional GANs: Application to segmenting brain tumours,” *Computers in Biology and Medicine*, vol. 170, p. 107982, 2024, doi: 10.1016/j.combiomed.2024.107982.
19. P. Friedrich, J. Wolleb, F. Bieder, A. Durrer, and P. C. Cattin, “WDM: 3D Wavelet Diffusion Models for High-Resolution Medical Image Synthesis,” in *MICCAI Workshop on Deep Generative Models*, 2024, pp. 11–21. doi: 10.1007/978-3-031-72744-3\_2.